

Energy-momentum tensor form factors of the nucleon in nuclear matter

Hyun-Chul Kim,^{1,2,3} Peter Schweitzer,² and Ulugbek Yakshiev¹

¹*Department of Physics, Inha University, Incheon 402-751, Republic of Korea*

²*Department of Physics, University of Connecticut, Storrs, CT 06269, U.S.A.*

³*School of Physics, Korea Institute for Advanced Study, Seoul 130-722, Republic of Korea*
(Dated: September, 2012)

The nucleon form factors of the energy-momentum tensor are studied in nuclear medium in the framework of the in-medium modified Skyrme model. We obtain a negative D -term, in agreement with results from other approaches, and find that medium effects make the value of d_1 more negative.

PACS numbers: 12.39.Fe, 12.39.Dc, 21.65.-f,

Keywords: Energy momentum tensor, Form factors, Nucleon, Chiral soliton, Nuclear matter

1. Understanding the structure of the nucleon has been one of fundamental issues well over decades. While the scalar, vector and axial-vector properties of the nucleon have been studied extensively and comprehended to a great extent, its energy-momentum tensor (EMT) form factors have been drawn to attention only quite recently, long after Pagels proposed them [1]. The reason can be found in the fact that it is very difficult to get direct access to these form factors experimentally. However, the generalized parton distributions (GPDs) [2–5], which are accessible via hard exclusive reactions [6–15], make it possible to extract information on the EMT form factors of the nucleon. In particular, certain Mellin moments of the GPDs can be expressed in terms of the EMT form factors [3, 16, 17].

The nucleon matrix element of the total symmetric EMT are parameterized by three form factors as follows [16, 17]

$$\langle p' | \hat{T}_{\mu\nu}(0) | p \rangle = \bar{u}(p', s') \left[M_2(t) \frac{P_\mu P_\nu}{M_N} + J(t) \frac{i(P_\mu \sigma_{\nu\rho} + P_\nu \sigma_{\mu\rho}) \Delta^\rho}{2M_N} + d_1(t) \frac{\Delta_\mu \Delta_\nu - g_{\mu\nu} \Delta^2}{5M_N} \right] u(p, s), \quad (1)$$

where $P = (p + p')/2$, $\Delta = (p' - p)$ and $t = \Delta^2$. M_N is the nucleon mass, and $u(p, s)$ denotes the nucleon spinor with the polarization vector s defined such that it is given as $(0, \mathbf{s})$ in the rest frame in which \mathbf{s} designates the axis of the spin quantization. The recent interest about the EMT form factors was stimulated by the fact that it is possible to define in QCD and to access in experiment the separate quark and gluon contributions to the form factors. The only presently known non-trivial piece of information is the decomposition of $M_2(t)$ at the zero-momentum transfer, which reveals that about 1/2 of the momentum of a fast moving nucleon is carried by quarks, and the other half by gluons. $J(t)$ provides analogous information on how the total angular momentum of quarks and gluons makes up the nucleon spin, but this information is presently not known. The interpretation of the last form factor $d_1(t)$ in Eq.(1) is less trivial but of equal significance for understanding the nucleon structure. It provides information on how the strong forces are distributed and stabilized in the nucleon [17, 18].

In all theoretical approaches where it was studied so far, $d_1 \equiv d_1(0)$ was found negative. This feature is expected to be deeply rooted in the spontaneous breakdown of chiral symmetry [19–21]. The form factor $d_1(t)$ can be extracted from the beam charge asymmetry in deeply virtual Compton scattering [20]. The EMT form factors of the nucleon have been studied in a variety of theoretical approaches: in lattice QCD [22–28], in chiral perturbation theory [30–34], in the chiral quark-soliton model [35–42] as well as in the Skyrme model [43]. Those of nuclei have also been studied [17, 44–46].

It is also of great importance to understand how the nucleon undergoes changes in nuclear matter. Studying the EMT form factors of the nucleon in medium offers a new perspective on the internal structure of the nucleon, and an important step towards the understanding of how nucleon properties are modified in nuclei. The first experimental study of deeply virtual Compton scattering on (gaseous) nuclear targets (H, He, N, Ne, Kr, Xe) was reported in [47]. The admittedly sizable error bars of this first experiment did not allow to observe nuclear modifications. More precise future experiments of this type can in principle provide information on nuclear modifications of EMT form factors.

Thus, in the present Letter, we aim at investigating the form factors of the total EMT of the nucleon in nuclear matter within the framework of an in-medium modified SU(2) Skyrme model, extending the previous work [43]. The Skyrme model [48, 49] provides a simple framework for the nucleon and connects chiral dynamics to the baryonic sector explicitly. Hence, the model can be easily extended to nuclear matter, modifications of chiral properties of the pion being taken into account. The changes of the nucleon in nuclear matter have been already examined within the in-medium modified Skyrme model [50, 51]. In Ref. [52], the model has been further elaborated, the stabilizing term being refined in medium, which we will take as our framework to study the EMT form factors of the nucleon in nuclear matter.

2. We start with the in-medium modified chiral Lagrangian [52]¹

$$\mathcal{L}^* = \frac{F_\pi^2}{16} \text{Tr}(\partial_0 U \partial^0 U^\dagger) - \alpha_p \frac{F_\pi^2}{16} \text{Tr}(\nabla U) \cdot (\nabla U^\dagger) + \frac{1}{32e^2\gamma} \text{Tr}[U^\dagger(\partial_\mu U), U^\dagger(\partial_\nu U)]^2 + \alpha_s \frac{m_\pi^2 F_\pi^2}{8} \text{Tr}(U - 2), \quad (2)$$

where U denotes the SU(2) pion field, F_π the pion decay constant, e a dimensionless parameter, and m_π the pion mass. The medium modifications are contained in the following functions [50–53]

$$\alpha_p(\rho) = 1 - \chi_p(\rho), \quad \chi_p(\rho) = \frac{4\pi c_0 \rho}{\eta + 4\pi c_0 g' \rho}, \quad \eta = 1 + \frac{m_\pi}{M_N} \quad (3)$$

$$\alpha_s(\rho) = 1 + \frac{\chi_s(\rho)}{m_\pi^2}, \quad \chi_s(\rho) = -4\pi\eta b_0 \rho, \quad (4)$$

$$\gamma(\rho) = \exp\left(-\frac{\gamma_{\text{num}}\rho}{1 + \gamma_{\text{den}}\rho}\right). \quad (5)$$

The $\alpha_{s,p}$ depend on the S - and P -wave pion-nucleus scattering lengths, volumes (b_0 and c_0), and the density ρ of nuclear matter [50, 53], and g' is the Lorentz-Lorenz or correlation parameter. Near the threshold, the energy dependence of b_0 and c_0 being ignored and nuclear matter being approximated to be homogeneous, $\alpha_{s,p}$ simply become functions of the given nuclear density. Similarly, the function γ in Eq.(5) describes the modification of the Skyrme term in nuclear matter proposed in Ref. [52] with γ_{num} and γ_{den} fitted to the coefficient of the volume term in the semiempirical mass formula. We can treat the modified chiral Lagrangian in terms of the renormalized effective constants $F_{\pi,t}^* = F_{\pi,t} = F_\pi$, $F_{\pi,s}^* = \alpha_p^{1/2} F_\pi$, $e^* = \gamma^{1/2} e$, and $m_\pi^* = (\alpha_s/\alpha_p)^{1/2} m_\pi$. The behavior of these parameters in nuclear matter is consistent with those in chiral perturbation theory [54] and QCD sum rules [55].

Homogeneous nuclear matter allows us to keep the hedgehog Ansatz for the pion field, i.e. $U = \exp[i\tau \frac{\mathbf{r}}{r} F(r)]$ with a profile function $F(r)$ in contrast to the case of local-density approximations for finite nuclei [56, 57]. Consequently, one can immediately write the classical mass functional as

$$M_{\text{sol}}^*[F] = 4\pi \int_0^\infty dr r^2 \left[\frac{F_{\pi,s}^{*2}}{8} \left(\frac{2 \sin^2 F}{r^2} + F'^2 \right) + \frac{\sin^2 F}{2e^{*2} r^2} \left(\frac{\sin^2 F}{r^2} + 2F'^2 \right) + \frac{m_\pi^{*2} F_{\pi,s}^{*2}}{4} (1 - \cos F) \right], \quad (6)$$

where $F' = dF/dr$. The minimization of the mass functional (6) leads to the equation for $F(r)$ as follows

$$\left(\frac{r^2}{4} + \frac{2F \sin^2 F}{e^{*2} F_{\pi,s}^{*2}} \right) F'' + \frac{rF'}{2} + \frac{F'^2 \sin 2F}{e^{*2} F_{\pi,s}^{*2}} - \frac{\sin 2F}{4} - \frac{\sin^2 F \sin 2F}{e^{*2} F_{\pi,s}^{*2} r^2} - \frac{m_\pi^{*2} r^2 \sin F}{4} = 0 \quad (7)$$

with the boundary conditions $F(0) = \pi$ and $F(r) \rightarrow 0$ as $r \rightarrow \infty$ imposed by the unit topological number of the chiral soliton. Having performed a collective quantization, we arrive at the modified collective Hamiltonian

$$H^* = M_{\text{sol}}^* + \frac{\mathbf{J}^2}{2\Theta^*} = M_{\text{sol}}^* + \frac{\mathbf{I}^2}{2\Theta^*}, \quad \Theta^* = \frac{2\pi}{3} \int_0^\infty dr r^2 s^2 \left[F_{\pi,t}^2 + \frac{4F'^2}{e^{*2}} + \frac{4s^2}{e^{*2} r^2} \right], \quad (8)$$

where \mathbf{J}^2 and \mathbf{I}^2 are the squared collective spin and isospin operators, respectively, which act on the nucleon or Δ wave functions obtained from the diagonalization of the collective Hamiltonian [49], and Θ^* is the moment of inertia of the soliton. A consistent description of the EMT form factors requires either to minimize the energy functional including rotational corrections, or to consider for the nucleon mass and other observables only the leading contribution in the limit of large number of colors N_c [43]. In this work we will follow Ref. [43] and choose the second option. In particular, this means that in our treatment the nucleon and Δ masses (in vacuum or in medium) are degenerate and given by the minimum of the mass functional (6).

Input parameters in the Skyrme sector are fixed as $m_\pi = 135$ MeV, $F_\pi = 108.78$ MeV, $e = 4.854$ following Ref. [52]. Those relevant to nuclear matter are determined by reproducing the coefficient of the volume term in the semiempirical mass formula and the experimental data for the compressibility of nuclear matter [52]: $b_0 = -0.024 m_\pi^{-1}$, $c_0 = 0.09 m_\pi^{-3}$, $g' = 0.7$, $\gamma_{\text{num}} = 0.797 m_\pi^{-3}$ and $\gamma_{\text{den}} = 0.496 m_\pi^{-3}$. All observables will be given as functions of ρ/ρ_0 with normal nuclear matter density $\rho_0 = 0.5 m_\pi^3$.

¹ From now on, the asterisks in expressions indicate the medium modified quantities which depend on the medium-dependent functions explicitly. Otherwise, we use the same symbol without any asterisk.

3. We are now in a position to calculate the EMT form factors of the nucleon in nuclear matter. Since the details of the general formalism have already been presented in Ref. [43] in free space, we briefly recapitulate only the necessary formulae here. The components of the static EMT [17] are given as follows:

$$T_{00}^*(r) = \frac{F_{\pi,s}^{*2}}{8} \left(\frac{2 \sin^2 F}{r^2} + F'^2 \right) + \frac{\sin^2 F}{2 e^{*2} r^2} \left(\frac{\sin^2 F}{r^2} + 2F'^2 \right) + \frac{m_{\pi}^{*2} F_{\pi,s}^{*2}}{4} (1 - \cos F), \quad (9)$$

$$T_{0k}^*(\mathbf{r}, \mathbf{s}) = \frac{\epsilon^{klm} r^l s^m}{(\mathbf{s} \times \mathbf{r})^2} \rho_J^*(r),$$

$$T_{ij}^*(\mathbf{r}) = s^*(r) \left(\frac{r_i r_j}{r^2} - \frac{1}{3} \delta_{ij} \right) + p^*(r) \delta_{ij}, \quad (10)$$

where T_{00}^* is called the energy density. The density of the angular momentum ρ_J^* , the pressure density, and the shear force density are expressed respectively as

$$\rho_J^*(r) = \frac{\sin^2 F}{12 \Theta^*} \left[F_{\pi,t}^2 + \frac{4}{e^{*2}} F'^2 + \frac{4}{e^{*2} r^2} \sin^2 F \right], \quad (11)$$

$$p^*(r) = -\frac{F_{\pi,s}^{*2}}{24} \left(\frac{2}{r^2} \sin^2 F + F'^2 \right) + \frac{\sin^2 F}{6 e^{*2} r^2} \left(\frac{\sin^2 F}{r^2} + 2F'^2 \right) - \frac{m_{\pi}^{*2} F_{\pi,s}^{*2}}{4} (1 - \cos F), \quad (12)$$

$$s^*(r) = \left(\frac{F_{\pi,s}^{*2}}{4} + \frac{1}{e^{*2} r^2} \sin^2 F \right) \left(F'^2 - \frac{1}{r^2} \sin^2 F \right). \quad (13)$$

The three form factors in Eq.(1) are finally given in the large N_c limit as

$$M_2^*(t) - \frac{t}{5M_N^{*2}} d_1^*(t) = \frac{1}{M_N^*} \int d^3\mathbf{r} T_{00}^*(r) j_0(r\sqrt{-t}), \quad (14)$$

$$d_1^*(t) = \frac{15M_N^*}{2} \int d^3\mathbf{r} p^*(r) \frac{j_0(r\sqrt{-t})}{t}, \quad (15)$$

$$J^*(t) = 3 \int d^3\mathbf{r} \rho_J^*(r) \frac{j_1(r\sqrt{-t})}{r\sqrt{-t}}, \quad (16)$$

where $j_0(z)$ and $j_1(z)$ represent the spherical Bessel functions of order 0 and 1, respectively. At the zero momentum transfer $t = 0$, $M_2^*(0)$ and $J^*(0)$ are normalized as

$$M_2^*(0) = \frac{1}{M_N^*} \int d^3\mathbf{r} T_{00}^*(r) = 1, \quad J^*(0) = \int d^3\mathbf{r} \rho_J^*(r) = \frac{1}{2}. \quad (17)$$

These relations were proven in [43] for a Skyrmion in free space, and we have checked that they hold also in nuclear matter. It is a feature of the approach with homogeneous nuclear matter that all expressions and proofs are formally analogous to the free nucleon case. In our approach, only the parameters of the Skyrme model are modified, but not the structure of the Lagrangian. (Of course, for a free nucleon the EMT is a Lorentz tensor. In nuclear medium we deal with a conserved Noether current.) Another important relation for $p^*(r)$ that is a consequence of the EMT conservation is the stability condition

$$\int_0^\infty dr r^2 p^*(r) = 0. \quad (18)$$

Again we verified that the analytic proofs of Eq. (18) formulated in [43] for a Skyrmion in free space can be carried over straightforwardly to the medium situation. Finally the constant d_1^* in nuclear matter is given by

$$d_1^* = 5\pi M_N^* \int_0^\infty dr r^4 p^*(r) = -\frac{4\pi M_N^*}{3} \int_0^\infty dr r^4 s^*(r) \quad (19)$$

The conservation of the EMT implies that $p^*(r)$ and $s^*(r)$ are connected to each other by the differential equation $\frac{2}{3} s'^*(r) + \frac{2}{r} s^*(r) + p'^*(r) = 0$ which is at the origin of the equivalent expressions for d_1^* in (19). We have checked that also in the medium-modified Skyrme model this differential equation holds, and the different expressions in Eq. (19) yield the same result for d_1^* , which is another demonstration of the theoretical consistency of the approach. Thus, the shear force density is directly related to the pressure density, so that we will concentrate only on the pressure here.

In the chiral quark-soliton model [41] it was observed that the negative sign of d_1 is a consequence of stability, which requires $p(r) > 0$ (repulsion) in the inner region, and $p(r) < 0$ (attraction) in the outer region, which must balance each other according to Eq. (18). By inserting a factor of r^2 in the stability integral (18) one basically obtains the expression for d_1 in Eq. (19) in terms of $p(r)$. The ‘‘additional factor’’ r^2 gives more weight to the outer region and is responsible for the negative sign of d_1 . This pattern was also observed for the Skyrmion in free space [43]. Below we will recover this picture, with important medium modifications.

4. We now proceed to present the results of the EMT form factors of the nucleon in nuclear matter and discuss their physical implications. In Table I, we list the quantities relevant to the EMT form factors and their densities. First we want to mention that the energy density in the center of the nucleon is rather sensitive to the input parameters in the Skyrmion sector. In fact, the energy density in the center of the nucleon in free space in this work turns out to be $T_{00}(0) = 1.45 \text{ GeV} \cdot \text{fm}^{-3}$, while $T_{00}(0) = 2.28 \text{ GeV} \cdot \text{fm}^{-3}$ was obtained in Ref. [43]. The reason lies in the different parameter set we use in the present approach.

As the density of the surrounding nuclear medium increases from zero to normal nuclear matter density, the energy density in the center of the nucleon decreases by about a factor of 2. At the same time we observe that the mean square radius for the energy density

$$\langle r_{00}^2 \rangle^* = \frac{\int d^3\mathbf{r} r^2 T_{00}^*(r)}{\int d^3\mathbf{r} T_{00}^*(r)} \quad (20)$$

increases. This implies that the nucleon is swollen in nuclear matter and its energy density spreads to larger distance in comparison with that in free space.

Let us more closely look into the change of the energy density in nuclear matter. The left panel of Fig. 1 shows how the energy density $T_{00}^*(r)$ changes in nuclear matter. We present in fact $4\pi r^2 T_{00}^*(r)$ normalized by the effective in-medium nucleon mass M_N^* such that the integration of the curve in the left panel of Fig. 1 yields unity. The solid curve draws it in free space, while the dashed and dotted ones depict those at $\rho = 0.5\rho_0$ and at normal density ($\rho = \rho_0$), respectively. Note that the nucleon mass M_N^* also changes as the density does. As ρ increases, the energy density gets weaker and shifted to the large distance. Moreover, at a finite ρ , it falls off more slowly than that in free space, as the distance r gets larger.

TABLE I: Different quantities related to the nucleon EMT densities and their form factors: $T_{00}^*(0)$ denotes the energy in the center of the nucleon; $\langle r_{00}^2 \rangle^*$ and $\langle r_J^2 \rangle^*$ depict the mean square radii for the energy and angular momentum densities, respectively; $p^*(0)$ represents the pressure in the center of the nucleon, whereas r_0^* designates the position where the pressure changes its sign; d_1^* is the value of the $d_1^*(t)$ form factor at the zero momentum transfer.

| ρ/ρ_0 | $T_{00}^*(0)$ [GeV · fm ⁻³] | $\langle r_{00}^2 \rangle^*$ [fm ²] | $\langle r_J^2 \rangle^*$ [fm ²] | $p^*(0)$ [GeV · fm ⁻³] | r_0^* [fm] | d_1^* |
|---------------|--|--|---|---------------------------------------|-----------------|---------|
| 0 | 1.45 | 0.68 | 1.09 | 0.26 | 0.71 | -3.54 |
| 0.5 | 0.96 | 0.83 | 1.23 | 0.18 | 0.82 | -4.30 |
| 1.0 | 0.71 | 0.95 | 1.35 | 0.13 | 0.90 | -4.85 |

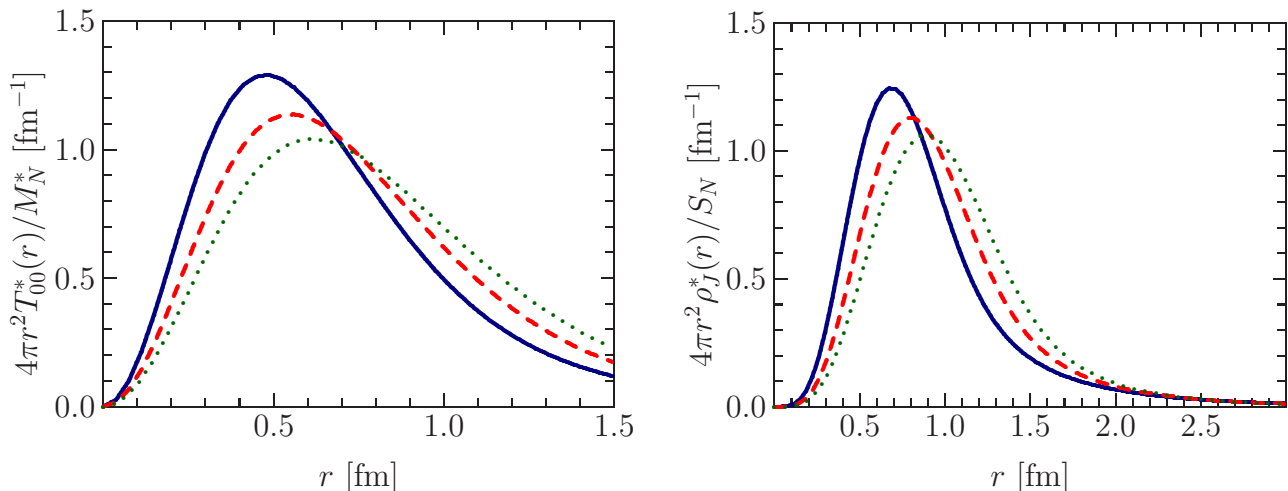


FIG. 1: (Color online) In the left panel, the energy densities of the nucleon normalized by the nucleon mass, $4\pi r^2 T_{00}^*(r)/M_N^*$, are presented as functions of r . The solid curve draws that in free space, whereas the dashed and dotted ones depict those at the density $\rho = 0.5\rho_0$ and at normal density ρ_0 , respectively. In the right panel, the densities of the angular momentum normalized by the nucleon spin $S_N = 1/2$, $4\pi r^2 \rho_J^*(r)/S_N$ are rendered as functions of r . The other notations are the same as in the left panel.

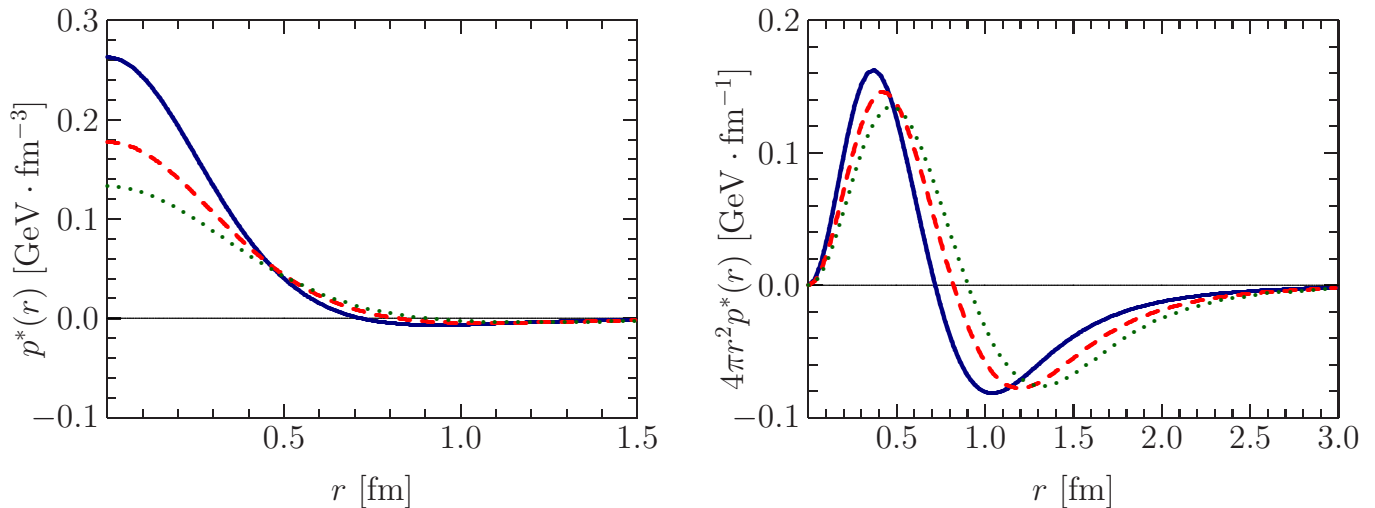


FIG. 2: (Color online) The pressure densities $p^*(r)$ and $4\pi r^2 p^*(r)$ as functions of r in the left and right panels, respectively. Notations are the same as in Fig. 1.

The density for the angular momentum $\rho_j^*(r)$, which is related to T_{0k}^* , vanishes in the center of the nucleon. The corresponding mean square radius $\langle r_j^2 \rangle^*$ which is defined analogously to $\langle r_{00}^2 \rangle^*$ in Eq. (20) starts to increase mildly as the density of nuclear matter increases as shown in Table I and exhibits similar behavior to $\langle r_{00}^2 \rangle^*$.

Knowing the pressure density is also of great significance, which contains information on the spatial components of the EMT. In the fifth column of Table I, we list the values of the pressure in the center of the nucleon, $p(0)^*$, given nuclear matter densities. It decreases with ρ increased. In the meanwhile, the position r_0^* , where the pressure changes the sign, becomes larger when ρ is switched on, which is in line with the features of the mean square radii discussed previously. That is, one can say that the shape of the nucleon is bulging out with nuclear matter.

Figure 2 shows how the pressure is distributed in the nucleon. As discussed already in Ref. [43], the positive sign of the pressure for $r < r_0$ indicates repulsion, while the negative one in the region $r > r_0$ signifies attraction. In the Skyrme model, the repulsive part is provided by the 4-derivative stabilizing (Skyrme) term, whereas the attractive one mainly comes from the kinetic term. Since the coefficient e is related to the vector meson coupling [59], such a distribution of the pressure can be interpreted as follows: While its repulsive part (or core part) is mainly governed by the vector mesons (ρ meson), the attractive part (or long-range part) is explained solely by the pions. This picture

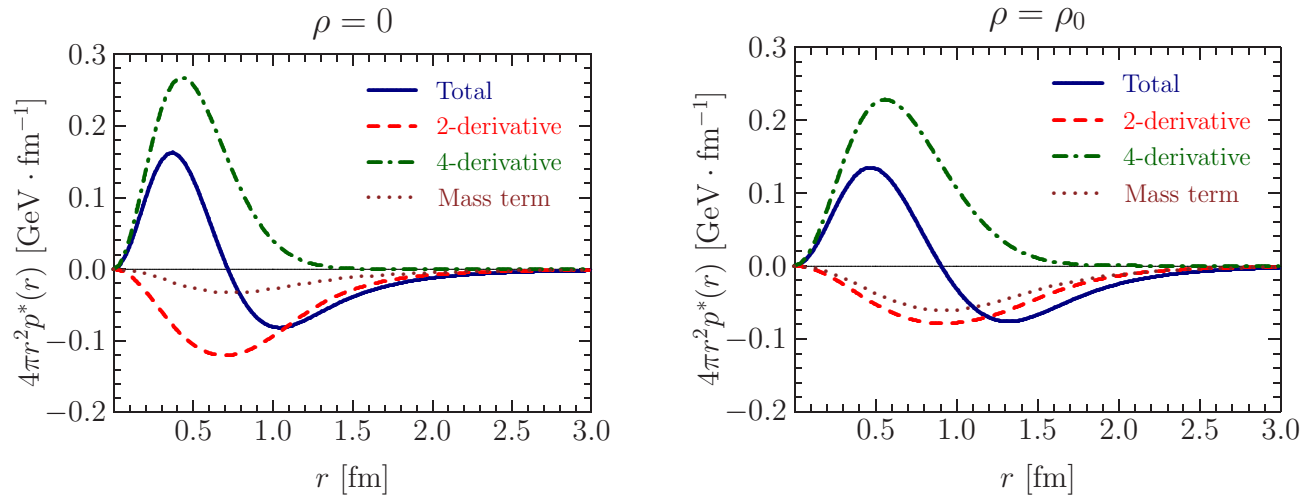


FIG. 3: (Color online) The decomposition of the pressure densities $4\pi r^2 p^*(r)$ as functions of r , in free space ($\rho = 0$) and at $\rho = \rho_0$, in the left and right panels, respectively. The solid curves denote the total pressure densities, the dashed ones represent the contributions of the 2-derivative (kinetic) term, the long-dashed ones are those of the 4-derivative (stabilizing) term, and the dotted ones stand for those of the pion mass term.

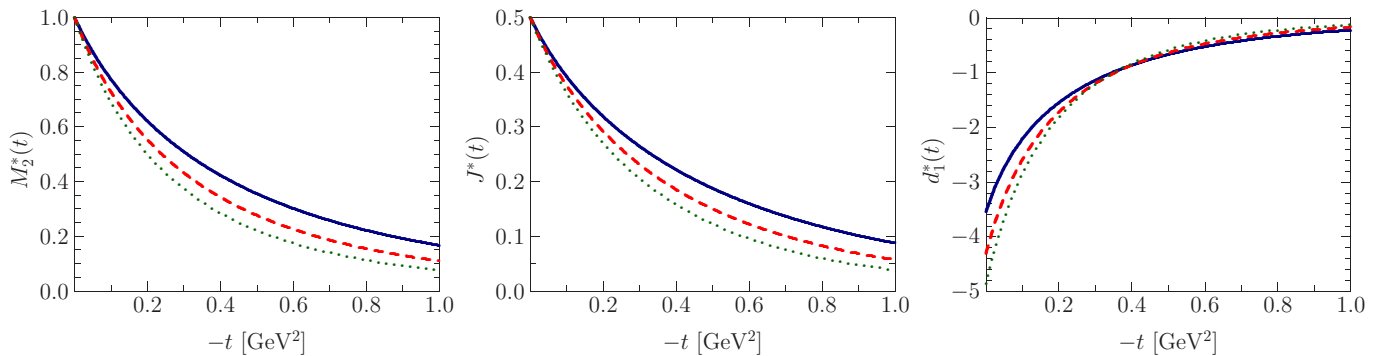


FIG. 4: (Color online) The EMT form factors of the nucleon $M_2^*(t)$, $J^*(t)$, and $d_1^*(t)$ as functions of t for the nucleon. Notations are the same as in Fig. 1.

is right also in nuclear matter, which is explained in Fig. 3. Comparing each contribution in the right panel ($\rho = \rho_0$) to the corresponding one in the left panel, we immediately realize that the 2- and 4-derivative terms are suppressed as well as stretched to larger distance. On the other hand, the mass term is enhanced at finite density. In order to understand this feature more precisely, we examine the expression for $p^*(r)$ given in Eq.(12). The relevant coefficient in the kinetic term is $F_{\pi,s}^*$ that becomes smaller as ρ increases, so that its contribution to $p^*(r)$ gets diminished. In the meanwhile, e^* governs the strength of the contribution of the stabilizing term. It grows as ρ is turned on, which leads to lessen the contribution of the stabilizing one to $p^*(r)$. In the case of the pion mass term contribution to $p^*(r)$, the pertinent coefficient is $m_\pi^{*2} F_{\pi,s}^{*2} = m_\pi^2 F_\pi^2 \alpha_s$, which becomes larger with ρ increased. That results in the enhancement of the pion mass term. While all these contributions undergo changes in nuclear matter, the stability condition of Eq. (18) is still satisfied. Integrating each contribution, we obtain for the case of free space:

$$\int_0^\infty dr r^2 p(r) = \begin{cases} -9.550 \text{ MeV} & \text{for the kinetic term} \\ 12.446 \text{ MeV} & \text{for the Skyrme term} \\ -2.896 \text{ MeV} & \text{for the pion mass term,} \end{cases} \quad (21)$$

whereas for the case of $\rho = \rho_0$

$$\int_0^\infty dr r^2 p^*(r) = \begin{cases} -7.741 \text{ MeV} & \text{for the kinetic term} \\ 13.652 \text{ MeV} & \text{for the Skyrme term} \\ -5.911 \text{ MeV} & \text{for the pion mass term.} \end{cases} \quad (22)$$

We see that adding up all contributions becomes zero, as required by the stability condition (18).

Having performed the Fourier transforms of the densities $T_{00}^*(r)$, $\rho_J^*(r)$, and $p^*(r)$ discussed so far, we immediately obtain the nucleon EMT form factors. Figure 4 draws the resulting EMT form factors as functions of t . The form factors $M_2^*(t)$ and $J^*(t)$ fall off more rapidly as ρ increases. On the other hand, $d_1^*(t)$ is rather distinguished from the other two form factors. While $M_2^*(t)$ and $J^*(t)$ are constrained to be 1 and 1/2 at $t = 0$ as shown in Eq. (17), $d_1^*(t)$ does not have such a constraint. However, had one scaled $d_1^*(t)$ so that their values may coincide at $t = 0$, $d_1^*(t)$ would have ended up with almost the same response to ρ as $M_2^*(t)$ and $J^*(t)$. As shown in Fig. 4, all the EMT form factors get stiffer near the zero momentum transfer, as the density of nuclear matter increases. It implies that all the corresponding radii get enlarged with ρ increased, as was already discussed for the case of $\langle r_{00}^2 \rangle^*$ and $\langle r_J^2 \rangle^*$.

All EMT form factors can be well approximated by dipole-type parametrizations $F^*(t) = F^*(0)/(1 - t/M_{F^*}^{*2})^2$ with the generic dipole masses M_{F^*} listed in Table II.

TABLE II: The dipole masses of the EMT form factors $M_2^*(t)$, $J^*(t)$ and $d_1^*(t)$ which approximate well the results in Fig. 4.

| ρ/ρ_0 | $M_{M_2^*}^*$ [GeV] | $M_{J^*}^*$ [GeV] | $M_{d_1^*}^*$ [GeV] |
|---------------|---------------------|-------------------|---------------------|
| 0 | 0.840 | 0.856 | 0.592 |
| 0.5 | 0.756 | 0.798 | 0.582 |
| 1.0 | 0.702 | 0.760 | 0.578 |

5. So far we have considered the medium effects in the range $0 \leq \rho \leq \rho_0$ where our approach based on linear response theory of pions in medium [53] is applicable. The description in terms of hadronic degrees of freedom is expected to become inappropriate and to break down at densities beyond ρ_0 . It is interesting to remark that by continuing our in-medium modified Skyrme model to $\rho > \rho_0$ we find indications for this expected breakdown. We would like to stress that we do not expect the naive extrapolation of the linear response in Eqs. (3, 4) to work quantitatively. However, the results are qualitatively insightful.

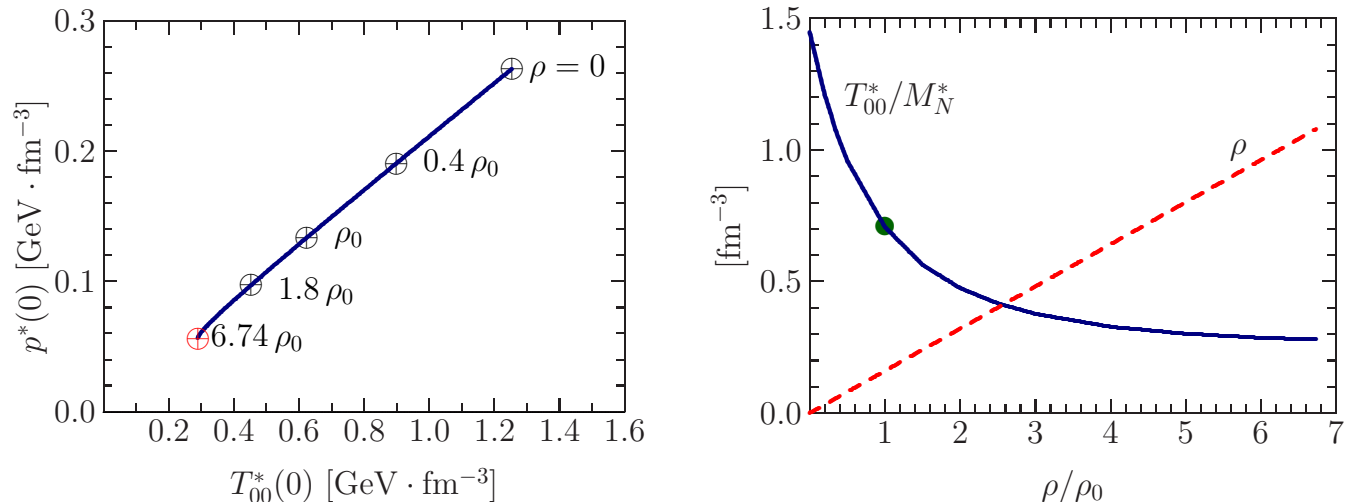


FIG. 5: (Color online) In the left panel, the correlated change of $p^*(0)$ and $T_{00}^*(0)$ are drawn with ρ varied. In the right panel, the T_{00}^*/M_N^* and ρ depicted as a function of ρ/ρ_0 . The maximal density is given as about $6.74\rho_0$, above which the Skyrmion does not exist anymore. The filled circle on the solid curve represents the value of T_{00}^*/M_N^* at normal nuclear matter density.

The left panel of Fig. 5 shows the correlated modifications of the pressure and energy densities in the center of the nucleon. We already have seen from Figs. 1 and 2, both $p^*(0)$ and $T_{00}^*(0)$ decrease as ρ grows. This trend continues also at higher densities, and the interesting point is that $p^*(0)$ and $T_{00}^*(0)$ are diminished at the same rate. This is natural if we consider nuclear matter density as an external parameter. The response of a stable system to variations of external parameters must be such that the pressure increases if the energy density does. The relation of $p^*(0)$ and $T_{00}^*(0)$ remains linear to a good approximation, until the Skyrmion ceases to exist at the “maximal nuclear density” $\rho_{\max} = 6.74\rho_0$. This maximal value arises because $\alpha_p(\rho) \rightarrow 0$ for $\rho \rightarrow \rho_{\max}$. In this limit the energy functional (6) has no minimum. This can be shown by means of the Derrick theorem [58], which is equivalent to the stability condition (18) [43]. In other words, in the limit $\rho \rightarrow \rho_{\max}$ the stability condition breaks down. We stress that this maximal density appears only in the mathematical description of our medium-modified Skyrmion, and has nothing to do with the physical critical point relevant to the restoration of chiral symmetry.

The fact that the Skyrmion ceases to exist as $\rho \rightarrow \rho_{\max}$ is of interest from a mathematical point of view. Of far greater relevance is that physical description of the nucleon in medium breaks down before this point is reached. This is because at $\rho \approx (2-3)\rho_0$ two things happen. Firstly, the normalized energy density $T_{00}^*(0)/M_N^*$ (alternatively one could also consider the baryon number density) becomes comparable with the density of the surrounding nuclear medium (see the right panel of Fig. 5). Secondly, the size of the nucleon, as measured for instance in terms of the square root of the mean square radii or r_0^* , becomes comparable to $\rho^{-1/3}$ which implies a spatial overlap of the nucleons in the nuclear medium. At this point it makes no sense anymore to mention an “individual nucleon” in nuclear medium, and a description in terms of more appropriate degrees of freedom becomes necessary (“quark matter”). It is very interesting to observe that the medium-modified Skyrme model signals in this way its limitations.

6. In the present work, we investigated the energy-momentum tensor form factors of the nucleon in nuclear matter, based on the in-medium modified Skyrme model. Employing all the parameters fixed in previous works, we derived the densities relevant to the energy, the angular-momentum, the pressure, and the shear-force distributions in the nucleon. We first examined how the energy and angular-momentum densities were modified in nuclear matter. In general their values in the center of the nucleon are suppressed but they are stretched to larger distance in nuclear matter. This was documented by the increase of the corresponding mean square radii with nuclear matter density.

We also analyzed the medium modifications of the pressure density. Again, its value in the center of the nucleon decreases as nuclear matter density grows. The change of the pressure density showed a similar behavior to the energy density in matter. The position where the pressure changes sign increases with nuclear matter density increased, and

the pressure density falls off in medium more slowly than that in free space. Since the pressure plays an essential role in the stability of the Skyrmion, we scrutinized each contribution of the kinetic, stabilizing, and mass terms. With nuclear matter density increased, the contributions of the kinetic and stabilizing terms are suppressed in magnitude, while that of the mass term becomes larger, and all contributions extend to larger distances. The stability condition was shown to be satisfied also in nuclear matter. Moreover in nuclear matter the constant d_1^* is negative as a consequence of stability. In particular, we observe that medium effects further decrease the value of d_1^* .

The energy-momentum tensor form factors $M_2(t)$ and $J(t)$, which are constrained to be 1 and 1/2 at zero momentum transfer, were found to fall off more rapidly as nuclear matter density increased. The absolute magnitude of the values of the $d_1^*(t)$ form factor increased in medium, compared to that in free space. The medium effects on its t -dependence were more or less similar to the other two form factors. Our results may pave a way towards a better understanding of the discrepancy between predictions obtained from different models of nuclei [17, 44, 45].

The present results for the modification of the EMT form factors and related properties, with nuclear density varied from zero to normal nuclear matter density and beyond that, indicate a breakdown of the description of the nucleon in nuclear matter densities at $\rho \approx (2-3)\rho_0$. At such high densities the nucleon in nuclear matter starts to lose its identity, and it would finally melt away, which implies that a description in different degrees of freedom becomes appropriate at such high densities.

Acknowledgments

The works of H.-Ch. K. and U. Y are supported by Basic Science Research Program through the National Research Foundation of Korea (NRF) funded by the Ministry of Education, Science and Technology (Grant Number: 2012004024 (H.-Ch. K.) and Grant Number: 2011-0023478 (U. Y.)), respectively. P. S. is supported by DOE contract No. DE-AC05-06OR23177, under which Jefferson Science Associates, LLC operates Jefferson Lab.

-
- [1] H. Pagels, Phys. Rev. **144** (1966) 1250.
 - [2] D. Müller, D. Robaschik, B. Geyer, F. M. Dittes and J. Hořejši, Fortsch. Phys. **42** (1994) 101.
 - [3] X. D. Ji, Phys. Rev. D **55** (1997) 7114.
 - [4] J. C. Collins, L. Frankfurt and M. Strikman, Phys. Rev. D **56** (1997) 2982.
 - [5] A. V. Radyushkin, Phys. Rev. D **56** (1997) 5524.
 - [6] P. R. B. Saull [ZEUS Collaboration], arXiv:hep-ex/0003030.
 - [7] C. Adloff *et al.* [H1 Collaboration], Phys. Lett. B **517** (2001) 47.
 - [8] A. Airapetian *et al.* [HERMES Collaboration], Phys. Rev. Lett. **87** (2001) 182001.
 - [9] S. Stepanyan *et al.* [CLAS Collaboration], Phys. Rev. Lett. **87** (2001) 182002.
 - [10] F. Ellinghaus [HERMES Collaboration], Nucl. Phys. A **711** (2002) 171.
 - [11] S. Chekanov *et al.* [ZEUS Collaboration], Phys. Lett. B **573** (2003) 46.
 - [12] A. Aktas *et al.* [H1 Collaboration], Eur. Phys. J. C **44** (2005) 1.
 - [13] A. Airapetian *et al.* [HERMES Collaboration], Phys. Rev. D **75** (2007) 011103.
 - [14] C. M. Camacho *et al.* [Jefferson Lab Hall A and Hall A DVCS Collaborations], Phys. Rev. Lett. **97** (2006) 262002.
 - [15] F. X. Girod *et al.* [CLAS Collaboration], Phys. Rev. Lett. **100** (2008) 162002.
 - [16] X. D. Ji, Phys. Rev. Lett. **78** (1997) 610.
 - [17] M. V. Polyakov, Phys. Lett. B **555** (2003) 57.
 - [18] M. V. Polyakov and A. G. Shuvaev, hep-ph/0207153.
 - [19] M. V. Polyakov and C. Weiss, Phys. Rev. D **60** (1999) 114017.
 - [20] N. Kivel, M. V. Polyakov and M. Vanderhaeghen, Phys. Rev. D **63** (2001) 114014.
 - [21] K. Goeke, M. V. Polyakov and M. Vanderhaeghen, Prog. Part. Nucl. Phys. **47** (2001) 401.
 - [22] N. Mathur, S. J. Dong, K. F. Liu, L. Mankiewicz and N. C. Mukhopadhyay, Phys. Rev. D **62** (2000) 114504.
 - [23] P. Hägler *et al.* [LHPC collaboration], Phys. Rev. D **68** (2003) 034505.
 - [24] M. Göckeler *et al.* [QCDSF Collaboration], Phys. Rev. Lett. **92** (2004) 042002.
 - [25] J. W. Negele *et al.*, Nucl. Phys. Proc. Suppl. **128** (2004) 170.
 - [26] D. Brommel *et al.* [QCDSF-UKQCD Collaboration], PoS LAT **2007** (2007) 158.
 - [27] J. D. Bratt *et al.* [LHPC Collaboration], Phys. Rev. D **82** (2010) 094502.
 - [28] K. F. Liu *et al.*, arXiv:1203.6388 [hep-ph].
 - [29] P. Hägler *et al.* [LHPC Collaboration], Phys. Rev. D **77** (2008) 094502.
 - [30] J. W. Chen and X. D. Ji, Phys. Rev. Lett. **88** (2002) 052003.
 - [31] A. V. Belitsky and X. D. Ji, Phys. Lett. B **538** (2002) 289.
 - [32] S. -I. Ando, J. -W. Chen and C. -W. Kao, Phys. Rev. D **74** (2006) 094013.

- [33] M. Diehl, A. Manashov and A. Schäfer, Eur. Phys. J. A **29** (2006) 315; Eur. Phys. J. A **31** (2007) 335.
- [34] M. Dorati, T. A. Gail and T. R. Hemmert, Nucl. Phys. A **798** (2008) 96.
- [35] V. Y. Petrov, P. V. Pobylitsa, M. V. Polyakov, I. Börnig, K. Goeke and C. Weiss, Phys. Rev. D **57** (1998) 4325.
- [36] P. Schweitzer, S. Boffi and M. Radici, Phys. Rev. D **66** (2002) 114004.
- [37] J. Ossmann, M. V. Polyakov, P. Schweitzer, D. Urbano and K. Goeke, Phys. Rev. D **71** (2005) 034011.
- [38] M. Wakamatsu and H. Tsujimoto, Phys. Rev. D **71** (2005) 074001.
- [39] M. Wakamatsu and Y. Nakakoji, Phys. Rev. D **74** (2006) 054006.
- [40] M. Wakamatsu, Phys. Lett. B **648** (2007) 181.
- [41] K. Goeke, J. Grabis, J. Ossmann, M. V. Polyakov, P. Schweitzer, A. Silva and D. Urbano, Phys. Rev. D **75** (2007) 094021.
- [42] K. Goeke, J. Grabis, J. Ossmann, P. Schweitzer, A. Silva and D. Urbano, Phys. Rev. C **75** (2007) 055207.
- [43] C. Cebulla, K. Goeke, J. Ossmann and P. Schweitzer, Nucl. Phys. A **794** (2007) 87.
- [44] V. Guzey and M. Siddikov, J. Phys. G **32** (2006) 251.
- [45] S. Liuti and S. K. Taneja, Phys. Rev. C **72** (2005) 032201.
- [46] S. Scopetta, Phys. Rev. C **79** (2009) 025207.
- [47] A. Airapetian *et al.* [HERMES Collaboration], Phys. Rev. C **81**, 035202 (2010) [arXiv:0911.0091 [hep-ex]].
- [48] T. H. R. Skyrme, Proc. Roy. Soc. Lond. A **260** (1961) 127.
- [49] G. S. Adkins, C. R. Nappi and E. Witten, Nucl. Phys. B **228** (1983) 552.
- [50] A. Rakhimov, M. M. Musakhanov, F. C. Khanna and U. T. Yakhshiev, Phys. Rev. C **58** (1998) 1738.
- [51] A. M. Rakhimov, F. C. Khanna, U. T. Yakhshiev and M. M. Musakhanov, Nucl. Phys. A **643** (1998) 383.
- [52] U. Yakhshiev and H.-Ch. Kim, Phys. Rev. C **83** (2011) 038203.
- [53] T. Ericson and W. Weise, *Pions and Nuclei* (Clarendon, Oxford, 1988).
- [54] U. G. Meissner, J. A. Oller and A. Wirzba, Ann. Phys. **297** (2002) 27.
- [55] H.c. Kim and M. Oka, Nucl. Phys. A **720** (2003) 368.
- [56] U. T. Yakhshiev, M. M. Musakhanov, A. M. Rakhimov, U. G. Meissner and A. Wirzba, Nucl. Phys. A **700** (2002) 403.
- [57] U. G. Meissner, A. M. Rakhimov, A. Wirzba and U. T. Yakhshiev, Eur. Phys. J. A **36** (2008) 37.
- [58] G. H. Derrick, J. Math. Phys. **11** (1964) 1252.
- [59] G. Ecker, J. Gasser, A. Pich and E. de Rafael, Nucl. Phys. B **321** (1989) 311.

